

Influence of Calcium Hydroxide Dissolution on the Transport Properties of Hydrated Cement Systems

by

Jacques Marchand ^{1,2}, Dale P. Bentz ³, Eric Samson ^{1,2} and Yannick Maltais ^{1,2}

**CRIB - Department of Civil Engineering ¹
Laval University, Canada, G1K 7P4**

**SIMCO Technologies, Inc. ²
1400 boul. Du Parc Technologique, Québec, Canada, G1P 4R7**

**Building and Fire Research Laboratory ³
National Institute of Standards and Technology
Gaithersburg, MD 20899 USA**

Reprinted from Materials Science of Concrete: Calcium Hydroxide in Concrete, Special Volume, Proceedings. American Ceramic Society. Workshop on the Role of Calcium Hydroxide in Concrete, November 1-3, 2000, Holmes Beach, Anna Maria Island, Florida, 113-129 pp., 2001.

NOTE: This paper is a contribution of the National Institute of Standards and Technology and is not subject to copyright.

NIST

National Institute of Standards and Technology
Technology Administration, U.S. Department of Commerce

INFLUENCE OF CALCIUM HYDROXIDE DISSOLUTION ON THE TRANSPORT PROPERTIES OF HYDRATED CEMENT SYSTEMS

Jacques Marchand^{1,2}, Dale Bentz³, Eric Samson^{1,2} and Yannick Maltais^{1,2}

¹CRIB - Department of Civil Engineering,
Laval University, Canada, G1K 7P4

²SIMCO Technologies Inc.,
1400 boul. du Parc Technologique, Québec, Canada, G1P 4R7

³Building and Fire Research Laboratory
National Institute of Standards and Technology, Gaithersburg, MD 20899, USA

ABSTRACT

Calcium hydroxide is one of the main reaction products resulting from the hydration of Portland cement with water. It is also one of the more soluble phases found in hydrated cement systems. The influence of calcium hydroxide dissolution and its effect on the diffusion properties of hydrated cement pastes were investigated using the NIST CEMHYD3D cement hydration and microstructure development model. The results of these simulations were implemented in another numerical model called STADIUM. This latter model can be used to predict the transport of ions in unsaturated porous systems. Numerical simulations clearly indicate that calcium hydroxide dissolution contributes to a marked increase in the porosity of the hydrated cement paste. This increase in porosity has a detrimental influence on the material transport properties. The results yielded by the numerical simulations are in good agreement with data of calcium leaching experiments performed in deionized water.

INTRODUCTION

Calcium hydroxide (CH), along with $C-S-H$, are the end products of the reaction of alite and belite with water. The abundance of CH in the hydrated cement paste varies with the degree of hydration of the cement, and can reach approximately 26% of the total volume of a mature paste. Contrary to the $C-S-H$ gel that is an ill-crystallized phase, CH is present predominantly in the form of well-defined crystals

To the extent authorized under the laws of the United States of America, all copyright interests in this publication are the property of The American Ceramic Society. Any duplication, reproduction, or republication of this publication or any part thereof, without the express written consent of The American Ceramic Society or fee paid to the Copyright Clearance Center, is prohibited.

in the hydrated cement paste. The size of these crystals tends to vary significantly from one to approximately 100 microns in diameter^{1,2}.

The leaching of calcium may be a matter of concern for the durability of concrete³. In some cases, CH dissolution and the decalcification of *C-S-H* may increase the porosity of the surface layers of concrete, and detrimentally affect the resistance of the material to deicer salt scaling and ion penetration⁴. In other instances, the leaching of calcium may also affect the core of the material and have a negative influence on the engineering properties of concrete structures³. For instance, CH dissolution and *C-S-H* decalcification have been found to have a detrimental influence on the mechanical and transport properties of hydrated cement systems⁵⁻⁹.

Over the years, several studies have clearly demonstrated that the investigation of calcium leaching mechanisms by laboratory experiments is often difficult and generally time-consuming^{8,9}. Furthermore, since both phenomena readily affect the pore structure of the material, the kinetics of CH dissolution and *C-S-H* decalcification quickly become non-linear, and a reliable prediction of the evolution of the concrete properties upon leaching can hardly be made on the sole basis of experimental results.

This paper presents the main results of a study of the influence of CH dissolution on the mechanisms of ion transport in hydrated cement systems. The effects of CH dissolution on the pore structure and transport properties of various hydrated cement paste mixtures were investigated using the NIST CEMHYD3D cement hydration and microstructure development model^{10,11}. These results were then implemented in another numerical model called STADIUM^{12,13}. This model can be used to predict the transport of ions and water in reactive porous materials (such as concrete). The degradation characteristics of neat cement paste mixtures immersed for 3 months in deionized water served as a basis for the validation of the model.

COMPUTER MODELING OF MICROSTRUCTURE AND DEGRADATION

Over the past decade, the development of numerical models has provided new tools to investigate the influence of calcium leaching on the evolution of the properties of cement-based materials. A few years ago, Bentz and Garboczi¹⁴ used a cellular automaton-type digital-image-based model to study the influence of CH dissolution on the pore structure of hydrated C_3S pastes. They showed that leaching mechanisms can have a detrimental effect on the connectivity of the pore structure of the material.

Table 1: Chemical and mineralogical properties of the three cements

Oxides	Cement		
	A: CSA Type 10	B: CSA Type 50	C: White
SiO ₂	19.78	21.45	24.29
Al ₂ O ₃	4.39	3.58	1.71
TiO ₂	0.22	0.21	0.07
Fe ₂ O ₃	3.00	4.38	0.32
CaO	62.04	63.93	68.60
SrO	0.26	0.07	0.13
MgO	2.84	1.81	0.54
Mn ₂ O ₃	0.04	0.05	0.03
Na ₂ O	0.32	0.24	0.14
K ₂ O	0.91	0.70	0.03
SO ₃	3.20	2.28	2.11
LOI	2.41	0.86	1.13
Bogue			
C ₃ S	59	62	77
C ₂ S	12	16	12
C ₃ A	7	2	4
C ₄ AF	9	13	1

The cement hydration and microstructure development model was later modified to account for the physical and mineralogical characteristics of cement grains on the properties of hydrated systems^{10,11}. This new model, called CEMHYD3D, was used to investigate the effects of CH dissolution on the pore structure and diffusion properties of two series of hydrated cement pastes prepared at w/c ratios of 0.4 and 0.6, respectively. Hydrated microstructures were created by considering the characteristics of three commercial cements (A: CSA Type 10, B: CSA Type 50 and C: a Danish white cement). The chemical and mineralogical properties of these cements are given in Table (1).

The starting three dimensional microstructures were based on the measured particle size distributions of the cement powders and two-dimensional SEM/X-ray image sets in which the clinker phases had been individually identified¹⁵. The starting microstructures were then hydrated either for 2000 cycles or until achieving a degree of hydration, α , that corresponded to the experimentally measured value (based on non-evaporable water measurements). The diffusivities of these "final" microstructures were then computed using the techniques described in the next section. These final microstructures were used as input microstructures for the leaching program. The CH in the microstructures was progressively leached as described previously¹⁴, and the diffusivity of the leached microstructures determined. In this way, the relative increase in diffusivity due to the leaching of CH from a hydrated microstructure could be assessed.

COMPUTATION OF DIFFUSIVITY

An electrical analogy is used to compute the relative diffusivity of the composite media¹⁶, where relative diffusivity is the ratio of the diffusivity of an ion in the composite media relative to its value in bulk water (proportional to the inverse of the formation factor). Conductivities are assigned to each phase comprising the microstructure and the resultant composite relative conductivity is computed¹⁷ and related to a relative diffusivity using the Nernst-Einstein relation¹⁶:

$$\frac{D}{D_0} = \frac{\sigma}{\sigma_0} \quad (1)$$

where σ/σ_0 is the computed relative conductivity and D/D_0 is the relative diffusivity for the random microstructure. For this study, capillary pores (ϕ) are assigned a relative diffusivity of 1.0, while the *C-S-H* gel is assigned a relative diffusivity of 0.0025 (1/400)¹⁷.

Previous studies have indicated that diffusivities computed using these relative values compare favorably to those measured experimentally¹⁷⁻¹⁸. For each hydrated/leached microstructure, the diffusivity was computed in each of the three principal directions and the average value reported.

MODELING IONIC TRANSPORT IN CEMENT SYSTEMS

As previously mentioned, the numerical results yielded by the NIST CEMHYD3D model were implemented in another model called STADIUM^{12,13}. This latter model has been developed to predict the transport of ions in unsaturated porous media. The model also accounts for the effect of dissolution/precipitation reactions on the transport mechanisms.

The description of the various transport mechanisms relies on the homogenization technique. This approach first requires writing all the basic equations at the microscopic level. These equations are then averaged over a Representative Elementary Volume (REV) in order to describe the transport mechanisms at the macroscopic scale^{19,20}.

In this model, ions are considered to be either free to move in the liquid phase or bound to the solid phase. The transport of ions in the liquid phase at the microscopic level is described by the extended Nernst-Planck equation²¹ to which is added an advection term. After integrating this equation over the REV, the transport equation

becomes:

$$\frac{\partial((1-\phi)C_{is})}{\partial t} + \frac{\partial(\theta C_i)}{\partial t} - \frac{\partial}{\partial x} \left(\theta D_i \frac{\partial C_i}{\partial x} + \theta \frac{D_i z_i F}{RT} C_i \frac{\partial \Psi}{\partial x} + \theta D_i C_i \frac{\partial \ln \gamma_i}{\partial x} - C_i V_x \right) = 0 \quad (2)$$

where the uppercase symbols represent the variables averaged over the REV. In equation (2), C_i is the concentration of the species i in the aqueous phase, C_{is} is the concentration in solid phase, θ is the volumetric water content (expressed in m^3/m^3 of material), D_i is the diffusion coefficient, z_i is the valence number of the species, F is the Faraday constant, R is the ideal gas constant, T is the temperature of the liquid, Ψ is the electrical potential, γ_i is the chemical activity coefficient and V_x is the velocity of the fluid. Equation (2) has to be written for each ionic species present in the system.

To calculate the chemical activity coefficients, several approaches are available. However, models such as those proposed by Debye-Hückel or Davies are unable to reliably describe the thermodynamic behavior of highly concentrated electrolytes such as the hydrated cement paste pore solution. A modification of the Davies equation described in reference²² was found to yield good results.

The Poisson equation is added to the model to evaluate the electrical potential Ψ . It relates the electrical potential to the concentration of each ionic species²³. The equation is given here in its averaged form:

$$\frac{\partial}{\partial x} \left(\theta \tau \frac{\partial \Psi}{\partial x} \right) + \theta \frac{F}{\epsilon} \sum_{i=1}^N z_i C_i = 0 \quad (3)$$

where N is the total number of ionic species, ϵ is the dielectric permittivity of the medium, in this case water, and τ is the tortuosity of the porous network.

The velocity of the fluid, appearing in equation (2) as V_x , can be described by a diffusion equation when its origin is in capillary forces present during drying/wetting cycles²⁴:

$$V_x = -D_w \frac{\partial \theta}{\partial x} \quad (4)$$

where D_w is the non-linear water diffusion coefficient. This parameter varies according to the water content of the material²⁴.

To complete the model, the mass conservation of the liquid phase must be taken into account²⁴:

$$\frac{\partial \theta}{\partial t} - \frac{\partial}{\partial x} \left(D_w \frac{\partial \theta}{\partial x} \right) = 0$$

As can be seen, moisture transport is described in terms of a variation of the (liquid) water content of the material. It should be emphasized that the choice of using the material water content as the state variable for the description of this problem has an important implication on the treatment of the boundary conditions. Since the latter are usually expressed in terms of relative humidity, a conversion has to be made. This can be done using an adsorption/desorption isotherm²⁴.

The first term on the left-hand side of equation (2) (in which C_{is} appears), accounts for the ionic exchange between the solution and the solid¹⁹. It can be used to model the influence of precipitation/dissolution reactions on the transport process. More information on this procedure can be found in reference¹².

The transport of ions and water in unsaturated cement systems can be fully described on the basis of equations (2) to (5). Previous experience¹² has shown that most practical problems can be reliably described by seven different ionic species (OH^- , Na^+ , K^+ , SO_4^{2-} , Ca^{2+} , $\text{Al}(\text{OH})_4^-$ and Cl^-) and five solid phases (CH, C-S-H, ettringite, gypsum and hydrogarnet).

The input data required to run the model can be easily obtained. The initial composition of the material (i.e. its initial content in CH, ettringite, ...) can be easily calculated by considering the chemical (and mineralogical) make-up of the binder, the characteristics of the mixture and the degree of hydration of the system²⁵.

The model also requires determining the initial composition of the pore solution and the porosity of the material. Samples of the pore solution of most hydrated cement systems can be obtained by extraction using the technique described by Longuet et al.²⁶. The total porosity of the material can easily be determined in the laboratory following standardized procedures (such as ASTM C642)²⁷.

Some information on the transport properties of the material is also required to run the model. The ionic diffusion properties of the solid can be determined by a migration test¹². The water diffusion coefficient of the material can be assessed by nuclear magnetic resonance imaging²⁴.

LEACHING EXPERIMENTS

In order to validate the results of the numerical simulations, six different cement paste mixtures were prepared with the three cements described in Table (1) and at two water/cement ratios (0.4 and 0.6). Only the results obtained for the 0.6 water/cement ratio mixture made of the CSA Type 10 cement (cement A) will be

reported. Data obtained for the other mixtures will be discussed in a forthcoming publication.

All mixtures were prepared using deionized water. The mixtures were batched in a high-speed mixer placed under vacuum (at 10 mbar) to prevent, as much as possible, the formation of air voids during mixing. Mixtures were cast in plastic cylinders (diameter = 7.0 cm, height = 20 cm). The molds were sealed and rotated for the first 24 hours in order to prevent any bleeding of the mixtures. At the end of this period, the cylinders were demoulded and sealed with an adhesive aluminum foil for an 18-month period at room temperature. This period was selected in order to get mature and well-hydrated cement pastes.

After the 18-month curing period, samples of each mixture were subjected to migration tests, porosity measurements pore solution extractions and thermal analyses (to assess the degree of hydration of each system). The experimental procedures for the migration tests and the pore solution extractions have been described elsewhere^{28,29}. Porosity measurements were carried out according to the requirements of ASTM C 642²⁷. The water diffusion properties of these mixtures had been previously determined by Nuclear Magnetic Resonance Imaging (NMRI) as part of a previous project³⁰.

The remaining parts of the cement paste cylinders were sawn in thin disks. The thickness of the disks varied from 12-15 mm. The disks were then vacuum saturated in a sodium hydroxyde solution (prepared at 300 mmol/l) for a 24-hour period prior to the degradation experiments. The latter were performed during three months under saturated (series 1) and unsaturated conditions (series 2) using deionized water.

The series 1 samples were first coated with an epoxy resin (on all their faces except one) and then immersed in the test solutions (see Figure (1)). For the samples of series 2 (unsaturated conditions), a relative humidity gradient was created between the two faces of the disks (see Figure (1)). One face was directly placed in contact with water and the other was placed in contact with a CO_2 free environment at a relative humidity close to 65%. In order to avoid carbonation, nitrogen was added on a daily basis in the compartment.

At the end of the degradation experiments, samples were broken in small pieces and then immersed in isopropyl (propan-2-ol) alcohol for a minimum period of 14 days. After this period, samples were dried under vacuum for 7 days. Once the drying process was completed, the samples were impregnated with an epoxy resin, polished, and coated with carbon.

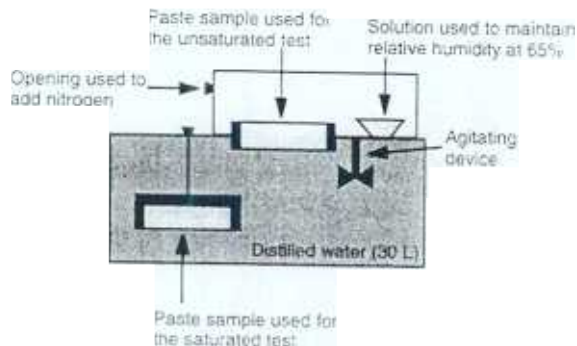


Figure 1: Degradation test set-up.

Microstructural alterations of the cement paste samples were investigated by means of electron microprobe analyses. The polished sections were observed using a microprobe (Cameca SX-100)¹ operating at 15 kV and 20 nA. For each sample, measurements were performed at a maximum interval of 13 microns on four distinct imaginary lines extending from the external surface in contact with the aggressive solution toward the internal part of the samples. At each point of measurement, the total content of calcium, sulfur, sodium, potassium, silicon, and aluminum was determined.

RESULTS AND DISCUSSION

Numerical results obtained with the NIST CEMHYD3D cement hydration and microstructure development model clearly indicate that leaching has a significant effect on the diffusivity of cement pastes. The diffusivity values calculated with the model for the original and completely leached microstructures are summarized in Table (2). In agreement with previous results for simpler C_3S systems¹⁴, the increase in diffusivity due to leaching is seen to be a factor of 20 or more, depending on the initial w/c ratio and the degree of hydration achieved prior to leaching. Additionally, the increase in diffusivity is seen to be much more dramatic for the lower w/c ratio systems, due mainly to the re-percolation of the capillary pore network during the leaching of the CH. For the higher w/c ratio systems, the depercolation of the

¹Certain commercial equipment is identified by name in this paper to adequately specify the experimental procedure. In no case does such identification imply endorsement by the National Institute of Standards and Technology, nor does it imply that the products are necessarily the best available for the purpose.

capillary porosity is never achieved during the initial hydration (since the critical percolation threshold for the capillary porosity is on the order of 0.20)^{14,17,18}. Thus, the relative increase in diffusivity caused by leaching is significantly less since both the hydrated and hydrated/leached microstructures contain a continuous capillary pore system.

Table 2: Model results for increase in diffusivity of cement pastes due to CH leaching

Cement	w/c	α	ϕ_{orig}	$(D/D_0)_{orig}$	ϕ_{leach}	$(D/D_0)_{leach}$	D_l/D_0
A	0.40	0.6823	0.216133	0.00465	0.365127	0.0726	15.62
A	0.40	0.7985	0.164761	0.00222	0.333371	0.0535	24.1
A	0.60	0.7234	0.383334	0.0647	0.502002	0.1877	2.90
A	0.60	0.8879	0.328439	0.0322	0.467383	0.1506	4.68
B	0.40	0.7141	0.200007	0.00338	0.346106	0.0569	16.86
B	0.40	0.8101	0.159915	0.00204	0.320229	0.0423	20.77
B	0.60	0.790	0.342954	0.0377	0.466465	0.141	3.74
B	0.60	0.9010	0.308901	0.0223	0.444681	0.1207	5.41
C	0.40	0.7364	0.188660	0.00286	0.353968	0.0617	21.57
C	0.40	0.8142	0.153031	0.0022	0.330547	0.0493	22.4
C	0.60	0.7583	0.356682	0.0438	0.489645	0.1689	3.86
C	0.60	0.8917	0.307971	0.0222	0.456563	0.1366	6.15

In addition to leaching all of the CH from a hydrated microstructure, a fraction of the CH can be leached by specifying a leaching probability and a number of leaching cycles to be executed in the leaching program. For each leaching cycle, the microstructure is first scanned to identify all CH pixels which are in contact with capillary porosity. In a second scan, these pixels are randomly leached in proportion to the user-specified leaching probability. For six of the microstructures summarized in Table (2), "partial" leaching of the microstructures has been executed. The results for the ratio of the diffusivity of the leached to that of the original hydrated microstructure as a function of the amount of CH leached are provided in Figure 2. As observed previously¹⁴ and in agreement with the available experimental data³⁰, initially the removal of a small portion of the CH due to leaching has only minor effects on the computed diffusivities. Then, as 30% to 60% of the CH is leached, the effects on diffusivity are more dramatic. Finally, above 90% leached, the increase in diffusivity tends to level off once more. Once again, it is clearly observed that the relative increase in diffusivity due to leaching is significantly greater for the lower 0.4 w/c ratio systems. Conversely, the differences between the three different cements at a constant w/c ratio are relatively minor, especially for CH leached fractions below about 50%.

In order to develop a simple equation for predicting the diffusivity ratio as a function of the fraction of CH leached from a microstructure, all of the data in Figure 2 were normalized using the diffusivity ratios for the original, ($DR(CH = 0)$), and

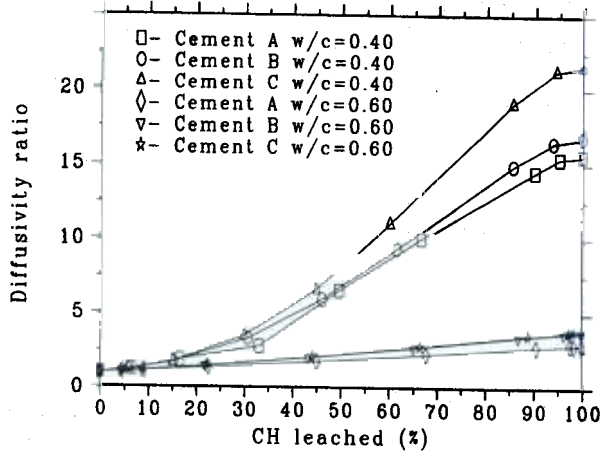


Figure 2: Model results for increase in diffusivity of cement pastes due to leaching of CH

completely leached, ($DR(CH = 100)$), microstructures and the following equation:

$$D_N(CH) = 1 + \frac{DR(CH) - DR(CH = 0)}{DR(CH = 100) - DR(CH = 0)} \quad (6)$$

It can be easily observed that this will result in normalized diffusivities (D_N) with values between 1 and 2 for every case.

These normalized diffusivity ratios are plotted vs. the fraction of CH leached for each of the six cement paste systems in Figure (3). While there is still some scatter amongst the different systems, particularly for small values of the CH leached, for engineering purposes, all of the data in Figure (3) has been fitted to the following equation:

$$D_N(CH) = 1 + \frac{1.1 \times CH^2}{0.28 + 0.79 \times CH} \quad (7)$$

where CH is the fraction of CH leached, having values in the range of [0,1]. As indicated by the dashed line in Figure (3), this equation gives an acceptable "average" fit to all of the data and will provide a simple method for estimating the diffusivity ratio for intermediate CH leaching when the values for the original and completely leached microstructures have been measured or computed.

Also included in Figure (3) are the upper and lower bounds computed using both the series/parallel and Hashin-Shtrikman equations³¹. In this case, it is assumed

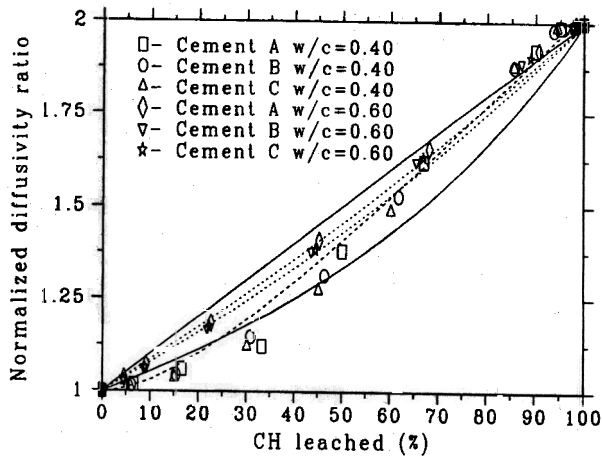


Figure 3: Model results for normalized diffusivity ratio as a function of amount of CH leached from the microstructure. Solid lines indicate series/parallel bounds for a simple two-phase composite, dotted lines are the Hashin-Shtrikman upper and lower bounds, and dashed line is the fit of equation 7 to all of the computer simulation data.

that the partially leached microstructure is composed of two components: original unleached cement paste with a normalized diffusivity of 1 and totally leached cement paste with a normalized diffusivity of 2. The fact that many of the plotted data points lie outside of these bounds (particularly the more restrictive Hashin-Shtrikman bounds) indicates that the simple consideration of a partially leached microstructure as a composite of unleached and totally leached phases is not totally appropriate but still serves as a useful abstraction.

The data provided by the NIST model were implemented in STADIUM and simulations were run for the 0.6 water/cement ratio mixture made of the CSA Type 10 cement (cement A) tested in saturated and unsaturated conditions. All the input data used in the simulations are summarized in Tables (3) and (4).

Results of the simulations are given in Figures (4) and (5). The total concentrations in calcium (expressed in g/kg of paste) yielded by the model are compared to the experimental calcium profiles provided by the microprobe analyses. The curve labeled "with damage factor" corresponds to the results calculated by taking into account the effect of CH dissolution on the transport properties of the paste mixtures (see Table (2) and Figure (2)). Microprobe data are given in counts per second (Cps).

Table 3: Physical characteristics of the two mixtures

Mixture	Diffusion coefficient (m ² /s)	Porosity (%)	α (%)	
W/C=0.40	OH ⁻	7.6e-11	37	68
	Na ⁺	1.9e-11		
	SO ₄ ²⁻	2.2e-11		
	K ⁺	2.8e-11		
	Ca ²⁺	1.1e-11		
W/C=0.60	OH ⁻	17.6e-11	52	75
	Na ⁺	4.5e-11		
	SO ₄ ²⁻	5.2e-11		
	K ⁺	6.5e-11		
	Ca ²⁺	2.6e-11		

Table 4: Pore solution chemistry

Ion	Concentration (mmol/L)	
	W/C = 0.40	W/C = 0.60
OH ⁻	700	434
Na ⁺	192	111
SO ₄ ²⁻	44	4
K ⁺	592	327
Ca ²⁺	2	2

As can be seen, whatever the moisture state of the samples, the calcium profiles predicted by the model are in good agreement with the profiles obtained by the microprobe analyses. Not only does the model accurately predict the depth of CH penetration, but it also reproduces quite well the total distribution in calcium over the entire thickness of the samples. It should be emphasized that the model has no "fitting parameter", and that the numerical simulations are solely based on the properties of the mixture and the chemical damage equation derived from numerical data provided by the NIST model. However, since the model predicts an averaged concentration per unit volume (or unit mass) of material, the numerical results do not reproduce the local variations in calcium measured by the microprobe analyses. These variations are due to the experimental "noise" of the technique and the presence of CH crystals within the hydrated cement paste matrix.

Both series of results also indicate that the increase in diffusivity induced by the removal of CH has a limited influence on the kinetics of degradation. This phenomenon can be explained by the fact that the duration of the experiments was

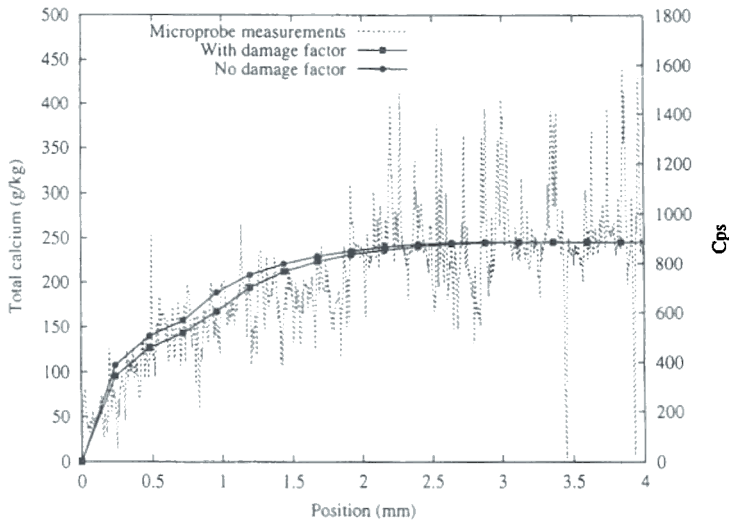


Figure 4: Total calcium profile after three months of immersion - CSA Type 10, W/C = 0.6, saturated conditions

limited to only 3 months. As can be seen, degradation is limited to the first two millimeters near the surface. For longer exposure periods (and thicker samples), the influence of CH dissolution would most certainly have a more significant effect on the degradation kinetics. Simulations ran for a 100-mm thick sample clearly indicate that chemical damage (i.e. the microstructural alterations induced by the dissolution of CH) does have a strong influence on the kinetics of penetration of the degradation front.

It should also be emphasized that experiments were carried out using a relatively porous mixture (prepared at a water/cement ratio of 0.6) which is less likely to be affected by the dissolution of CH. As previously mentioned, the pore structure of the 0.6 water/cement ratio mixture was already percolated, thus reducing the detrimental influence of CH dissolution on the transport properties of the material.

Additional simulations were run for the 0.4 water/cement ratio mixture prepared with the CSA Type 10 cement (cement A). Numerical results are given in Figure (6). Although the relative increase in diffusivity caused by leaching was found to be significantly more important for the 0.4 water/cement ratio mixtures, both series of results are similar. This phenomenon can be explained by the fact that the initial diffusion coefficient of the 0.4 water/cement ratio mixture was low,

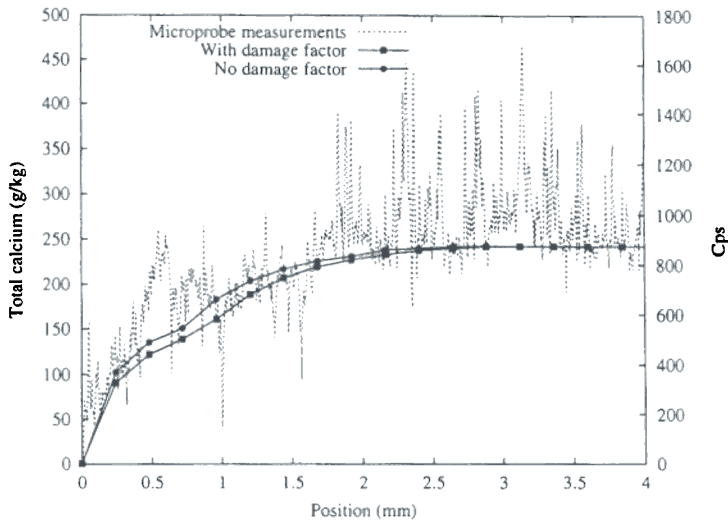


Figure 5: Total calcium profile after three months of exposure - CSA Type 10, W/C = 0.6, unsaturated conditions

thus reducing the rate of diffusion of calcium and hydroxide ions out of the sample. As can be seen in the figure, degradation is mainly limited to the first millimeter near the surface. These results clearly emphasize the importance of the diffusion coefficient of the material on the kinetics of degradation.

CONCLUDING REMARKS

The dissolution of CH was found to have a significant effect on the diffusivity of hydrated cement pastes. The increase in diffusivity due to leaching is seen to be a factor of 20 or more, depending on the initial w/c ratio and the degree of hydration achieved prior to leaching.

The increase in diffusivity is seen to be much more dramatic for the lower w/c ratio systems, due mainly to the re-percolation of the capillary pore network during the leaching of the CH.

Degradation profiles computed using the chemical damage equation provided by the NIST model and STADIUM compare favorably to experimental values.

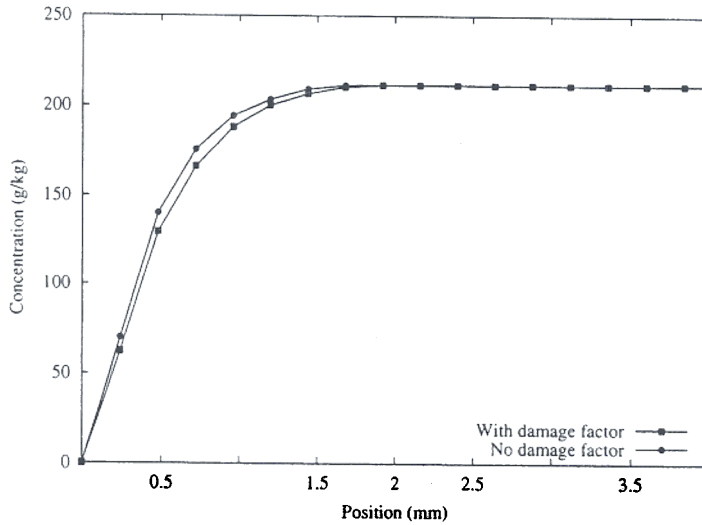


Figure 6: Total calcium profile after three months of immersion - CSA Type 10 W/C = 0.4

ACKNOWLEDGEMENTS

The authors are grateful to the Natural Sciences and Engineering Research Council of Canada and to SIMCO Technologies inc. for their financial support for this project.

REFERENCES

- ¹ St-John, D.A., Poole, A.W., Sims, I. (1998), *Concrete petrography - A handbook of investigative techniques*, Arnold , London, UK.
- ² Berger, R.L., McGregor, J.D. (1972), *Influence of admixtures on the morphology of calcium hydroxide formed during tricalcium silicate hydration*, Cement and Concrete Research, Vol. 2, pp. 43-55.
- ³ Marchand, J., Beaudoin, J.J., Pigeon, M. (1999), *Influence of $\text{Ca}(\text{OH})_2$ dissolution on the properties of cement systems*, Materials Science of Concrete - Sulfate Attack Mechanisms, American Ceramic Society, pp. 283-293.
- ⁴ Marchand, J., Pleau, R., Gagne, R. (1995), *Deterioration of concrete due to freezing and thawing*, Materials Science of Concrete, Vol. IV, American Ceramic Society, pp. 283-354.
- ⁵ Terzaghi, R.D. (1948), *Concrete deterioration in a shipway*, Journal of the

American Concrete Institute, Vol. 44, No. 6, pp. 977-1005.

⁶ Tremper, B. (1931), *The effects of acid waters on concrete*, Journal of the American Concrete Institute, Vol. 28, No. 9, pp. 1-32.

⁷ Carde, C., François, R. (1997), *Effect of the leaching of calcium hydroxide from cement paste on the mechanical and physical properties*, Cement and Concrete Research, Vol. 27, pp. 539-550.

⁸ Adenot, F., Buil, M. (1992), *Modelling the corrosion of the cement paste by deionized water*, Cement and Concrete Research, Vol. 22, pp. 489-496.

⁹ Delagrave, A., Gerard, G., Marchand, J. (1997), *Modelling calcium leaching mechanisms in hydrated cement pastes*, in Mechanisms of Chemical Degradation of Cement-Based Materials, E & FN Spon, pp. 38-49.

¹⁰ Bentz, D.P. (1997), *Three-dimensional computer simulation of cement hydration and microstructure development*, Journal of the American Ceramic Society, Vol. 80, No. 1, pp. 3-21.

¹¹ Bentz, D.P. (2000), *CEMHYD3D: A three-dimensional cement hydration and microstructure development modelling package. Version 2.0*, NISTIR 6485, U.S. Department of Commerce.

¹² Marchand, J. (2000), *Modeling the behavior of unsaturated cement system-exposed to aggressive chemical environments*, Materials and Structures, (in press).

¹³ Samson, E. (2000), *Modeling ion transport mechanisms in unsaturated cement systems*, Ph. D. thesis, Department of Civil Engineering, Laval University, Canada, (in preparation).

¹⁴ Bentz, D.P., Garboczi, E.J. (1992), *Modelling the leaching of calcium hydroxide from cement paste: Effects on pore space percolation and diffusivity*, Materials and Structures, Vol. 25, pp. 523-533.

¹⁵ Bentz, D.P., Stutzman, P.E. (1994), *SEM analysis and computer modelling of hydration of portland cement particles*, in Petrography of Cementitious Systems, ASTM STP-1215, Ed. S.M. DeHayes and D. Stark, American Society for Testing and Materials, Philadelphia, pp. 60-73.

¹⁶ Garboczi, E.J. (1998), *Finite element and finite difference programs for computing the linear electric and elastic properties of digital images of random materials*, NISTIR 6269, U.S. Department of Commerce, (see <http://ciks.cbt.nist.gov/monograph/>, Chapter 2).

¹⁷ Garboczi, E.J., Bentz, D.P. (1992), *Computer simulation of the diffusivity of cement-based materials*, Journal of Materials Science, Vol. 27, pp. 2083-2092.

¹⁸ Bentz, D.P., Jensen, O.M., Glasser, F.P., Coats, A.M. (2000), *Influence of silica fume on diffusivity in cement-based materials - Part I: Experimental and computer modelling studies on cement pastes*, Cement and Concrete Research, Vol. 30, pp 953-962.

¹⁹ Bear, J., Bachmat, Y. (1991), *Introduction to modeling of transport phenomena in porous media*, Kluwer Academic Publishers, The Netherlands.

²⁰ Samson, E., Marchand, J., Beaudoin, J.J. (1999), *Describing ion diffusion mechanisms in cement-based materials using the homogenization technique*, Cement and Concrete Research, Vol. 29, No. 8, pp.1341-1345.

²¹ Helfferich, F. (1962), *Ion exchange*, McGraw-Hill, New York, USA, 624 p.

²² Samson, E., Lemaire, G., Marchand, J., Beaudoin, J.J., (1999), *Modeling chemical activity effects in strong ionic solutions*, Computational Materials Science, Vol. 15, pp. 285-294.

²³ Samson, E., Marchand, J., Robert, J.L., Bournazel, J.P. (1999), *Modeling the mechanisms of ion diffusion transport in porous media*, International Journal of Numerical Methods in Engineering, Vol. 46, pp. 2043-2060.

²⁴ Pel, L. (1995), *Moisture transport in porous building materials*, Ph. D. thesis, Eindhoven University of Technology, The Netherlands, 125 p.

²⁵ Taylor, H.F.W. (1990), *Cement chemistry*, Academic Press Inc., San Diego, USA

²⁶ Longuet, P., Burglen, L., Zelwer, A. (1980), *The liquid phase of hydrated cement*, Publication Technique CERILH, Vol. 219, (in French).

²⁷ Jacobsen, S., Marchand, J., Boisvert, L. (1996), *Effect of cracking and healing on chloride transport in OPC concrete*, Cement Concrete Research, Vol. 26, No. 6, pp. 869-882.

²⁸ Diamond, S. (1981), *Effects of two Danish fly ashes on alkali contents of pore solutions of cement fly ash pastes*, Cement and Concrete Research, Vol. 11, No. 2, pp. 383-390.

²⁹ Hazrati, K. (1995), *Investigation of the mechanisms of moisture transport by capillary suction in ordinary and high-performance cement-based materials*, Ph. D. thesis, Laval University, Canada, 205 p.

³⁰ Revertegat, E., Richet, C., Gegout, P. (1992), *Effect of pH on the durability of cement pastes*, Cement and Concrete Research, Vol. 22, pp. 259-272.

³¹ Kuntz, M., Mareschal, J.C., Lavallee, P. (1997), *Numerical estimation of the effective conductivity of heterogeneous media with a 2D cellular automaton fluid*, Geophysical Research Letters, Vol. 24, No. 22, pp. 2865-2868, online at: <http://www.agu.org/GRL/articles/97GL52856/GL136W01.html>.